Aging underdamped scaled Brownian motion: Ensemble- and time-averaged particle displacements, nonergodicity, and the failure of the overdamping approximation

Hadiseh Safdari,[1,2] Andrey G. Cherstvy,[1] Aleksei V. Chechkin,[1,3,4] Anna Bodrova,[5,6] and Ralf Metzler[1,*]

[1]*Institute for Physics & Astronomy, University of Potsdam, 14476 Potsdam-Golm, Germany*
[2]*Department of Physics, Shahid Beheshti University, 19839 Tehran, Iran*
[3]*Institute for Theoretical Physics, Kharkov Institute of Physics and Technology, 61108 Kharkov, Ukraine*
[4]*Department of Physics & Astronomy, University of Padova, "Galileo Galilei" - DFA, 35131 Padova, Italy*
[5]*Institute of Physics, Humboldt University Berlin, 12489 Berlin, Germany*
[6]*Faculty of Physics, M. V. Lomonosov Moscow State University, 119991 Moscow, Russia*

We investigate both analytically and by computer simulations the ensemble- and time-averaged, nonergodic, and aging properties of massive particles diffusing in a medium with a time dependent diffusivity. We call this stochastic diffusion process the (aging) underdamped scaled Brownian motion (UDSBM). We demonstrate how the mean squared displacement (MSD) and the time-averaged MSD of UDSBM are affected by the inertial term in the Langevin equation, both at short, intermediate, and even long diffusion times. In particular, we quantify the ballistic regime for the MSD and the time-averaged MSD as well as the spread of individual time-averaged MSD trajectories. One of the main effects we observe is that, both for the MSD and the time-averaged MSD, for superdiffusive UDSBM the ballistic regime is much shorter than for ordinary Brownian motion. In contrast, for subdiffusive UDSBM, the ballistic region extends to much longer diffusion times. Therefore, particular care needs to be taken under what conditions the overdamped limit indeed provides a correct description, even in the long time limit. We also analyze to what extent ergodicity in the Boltzmann-Khinchin sense in this nonstationary system is broken, both for subdiffusive and superdiffusive UDSBM. Finally, the limiting case of ultraslow UDSBM is considered, with a mixed logarithmic and power-law dependence of the ensemble- and time-averaged MSDs of the particles. In the limit of strong aging, remarkably, the ordinary UDSBM and the ultraslow UDSBM behave similarly in the short time ballistic limit. The approaches developed here open ways for considering other stochastic processes under physically important conditions when a finite particle mass and aging in the system cannot be neglected.

I. INTRODUCTION

Anomalous diffusion processes feature a nonlinear growth of the ensemble-averaged mean squared displacement (MSD) of particles with time [1–13], namely,

$$\langle x^2(t) \rangle = \int_{-\infty}^{\infty} x^2 P(x,t) dx \sim 2K_\alpha t^\alpha. \qquad (1)$$

Here, $P(x,t)$ is the probability density function (PDF) to find the tracer particle at time t at position x and K_α is the generalized diffusion coefficient with physical dimensions $[K_\alpha] = \mathrm{cm}^2 \sec^{-\alpha}$. The anomalous, and in general time local, scaling exponent $\alpha(t)$ distinguishes the regimes of subdiffusive $(0 < \alpha < 1)$, normal $(\alpha = 1)$, and superdiffusive $(\alpha > 1)$ particle motions. The ballistic regime corresponds to $\alpha = 2$. An explicit time dependence of the scaling exponent $\alpha(t)$ indicates that a transient non-Brownian growth of the MSD occurs in the relevant time window (see, e.g., [14,15]). Hyperballistic MSD growth with $\alpha > 2$ can occur, for instance, for particle diffusion in turbulent flows [16,17] or for nonequilibrium initial conditions [18].

Anomalous particle kinetics was detected in numerous physical and biophysical systems. From the perspective of crowded [19–25] biological cells, the list of examples includes protein diffusion in living cells [26–29], motion of chromosomal loci [30–33] and polymeric molecules [34], diffusion of virus particles [35], motion of lipid and insulin granules inside cells [36,37], diffusion of membrane lipids [38–46] and membrane-crowding proteins [14,15,47,48], dynamics of ion channels [49–52] in biomembranes, diffusion of small molecules near cell membranes [53–55] and their permeation across membranes [56], active transport in cells [57–61], and, finally, the motion on the level of entire microorganisms [62].

In contrast to the universal Gaussian normal diffusion, anomalous diffusion processes are nonuniversal. There exist a variety of theoretical models sharing the same form (1) of the MSD [11], including continuous time random walks describing diffusion with a divergent waiting time scale [63–68] and trapping models in random energy landscapes [69–77]. In addition, models for particle motion in heterogeneous environments [78–86] and stochastic processes with distributed or time varying diffusion coefficient were considered [87–89]. Exponentially fast [90–92] and logarithmically slow [10,93–97] anomalous diffusion processes are also worth mentioning here. Moreover, fractional Brownian motion and fractional Langevin equation motion with a power-law correlated noise [98–100] can describe the dynamics of particles in viscoelastic media such as the cell cytoplasm. Also, correlated continuous time random walks should be mentioned here [101–103]. The adequate description of some systems required the coupling of more than one anomalous diffusion mechanism [36,37,49].

Here, we consider the remaining popular anomalous diffusion model, scaled Brownian motion (SBM), with the time dependent diffusion coefficient of the power-law

*rmetzler@uni-potsdam.de

form [104–109]

$$D(t) = \alpha K_\alpha t^{\alpha-1}. \tag{2}$$

SBM is a Gaussian and inherently nonstationary process. The power-law dependence (2) of the particle diffusivity was widely used to describe i.a. subdiffusion in cellular fluids [110], water diffusion in cells [111], and it naturally arises for the self-diffusion in granular gases [109,112,113]. For more examples, the reader is refereed to our recent study [109]. The exponent of $D(t)$ is $0 < \alpha < 1$ for subdiffusion, $1 < \alpha$ for superdiffusion, and $\alpha = 0$ denotes ultraslow SBM diffusion (considered in Ref. [96]). Note that nonstationary processes with a fluctuating two-state diffusion coefficient were quantified in Refs. [88,114,115] in terms of both the MSD and the time-averaged MSD. The overdamped approximation appears to work well there. The diffusion of massive particles experiencing a fluctuating friction was already studied in detail in Refs. [116].

Despite a great interest in the SBM process, the standard approaches usually deal with *massless* particles, the overdamped limit of the Langevin equation [11]. The regime of underdamped motion, when the inertial term is non-negligible [117], is typically less studied for anomalous diffusion processes. As exceptions we mention the fractional Langevin and fractional Klein-Kramers equations studied in Refs. [60,61,118–121]. In this case, under the conditions of weak coupling of particles to the thermal bath, the ballistic diffusion is known to govern the short time dynamics [122–124].

Recently, the first results for the underdamped SBM (UDSBM) process were obtained by the authors in Ref. [109]. It was found [109] that for $\alpha > 1$ the overdamped regime is reached rather soon, while for small positive α values an intermediate regime for the particle dynamics emerges and influences the particle dynamics, both for the MSD and the time-averaged MSD. Finally, for ultraslow SBM at $\alpha = 0$ the overdamped limit is not reached at all. Thus, a finite particle mass affects the dynamics at all time scales [109] and the description in terms of the conventional overdamped limit fails [96]. This present study clarifies which properties of UDSBM introduced in Ref. [109] should be modified in the presence of aging. The latter means that one starts recording the particle position after some aging time t_a. The current investigation involves some advanced computations and discovers additional diffusion regimes, as compared to nonaging UDSBM [109]. In particular, we derive scaling relations in the regime of strong aging in the system for the MSD, time-averaged MSD, and ergodicity breaking parameter.

For out-of-equilibrium processes such as SBM one expects severe effects of aging onto the particle dynamics [125,126]. Therefore, the time interval t_a impacts the statistical properties [11,127,128]. Effects of aging are observed, for instance, in glassy systems [129–133], homogeneously cooled granular fluids [134], for diffusion in plasma cell membranes [49,135], protein dynamics [136,137], in polymeric semiconductors [138], as well as for blinking statistics of quantum dots [139,140].

We here generalize the stochastic SBM process to the underdamped and aging situation. In Sec. II we introduce the observables and describe the routine for computer simulations. In Sec. III we present the main findings for the MSD, the time-averaged MSD, and the ergodicity breaking parameter of

aging UDSBM. The cases of subdiffusion and superdiffusion are considered separately. We compare the results of analytical calculations and extensive computer simulations in different aging regimes. In Sec. IV the MSD and the time-averaged MSD for the spatial case of ultraslow UDSBM are considered. In Sec. V we discuss some applications of our results and conclude.

II. OBSERVABLES AND SIMULATIONS MODEL

In addition to the standard characteristic of particle spreading given by the ensemble-averaged MSD [1], we are interested hereafter also in the the time-averaged MSD. The latter is defined from a single particle trajectory $x(t)$ as [11]

$$\overline{\delta^2(\Delta)} = \frac{1}{T-\Delta} \int_0^{T-\Delta} [x(t+\Delta) - x(t)]^2 dt. \tag{3}$$

The extension to higher dimensions is straightforward. Here, the lag time Δ is the width of the sliding window and T is the total trajectory length. Expression (3) is the standard measure to quantify particle displacements in single particle tracking experiments, when few but long time series $x(t)$ are typically available [141]. It is complementary to the ensemble-averaged MSD, widely used in the theoretical analysis of stochastic processes: there the averaging is performed at each time t over the ensemble of N given trajectories of the same length.

When the measurement starts after time t_a from the initiation of the process, the aging time-averaged MSD is naturally defined as [66–68]

$$\overline{\delta_a^2(\Delta)} = \frac{1}{T-\Delta} \int_{t_a}^{T+t_a-\Delta} [x(t+\Delta) - x(t)]^2 dt. \tag{4}$$

The average over N realizations of the diffusion process yields the *mean* time-averaged MSD,

$$\left\langle \overline{\delta^2(\Delta)} \right\rangle = \frac{1}{N} \sum_{i=1}^N \overline{\delta_i^2(\Delta)}, \tag{5}$$

and analogously for $\left\langle \overline{\delta_a^2(\Delta)} \right\rangle$. This trajectory based averaging gives rise to a smoother variation of the time-averaged MSD with the lag time, as compared to individual realizations (3). Note that for stochastic processes with a pronounced *scatter* of individual time-averaged MSD realizations, the determination of the mean (5) requires a substantial averaging sample to be generated [11].

For ergodic diffusion processes in the Boltzmann-Khinchin sense the MSD (1) and the time-averaged MSD (3) coincide in the limit $\Delta/T \ll 1$ [11]. A quantitative measure of the ergodic properties of a stochastic process [142–146] is the ergodicity breaking parameter, EB, defined via the fourth moment of the time-averaged MSD [98,147]

$$\mathrm{EB}(\Delta) = \frac{\left\langle [\overline{\delta^2(\Delta)}]^2 \right\rangle - \left\langle \overline{\delta^2(\Delta)} \right\rangle^2}{\left\langle \overline{\delta^2(\Delta)} \right\rangle^2} = \langle \xi^2(\Delta) \rangle - 1. \tag{6}$$

Here, the ratio

$$\xi(\Delta) = \frac{\overline{\delta^2(\Delta)}}{\left\langle \overline{\delta^2(\Delta)} \right\rangle} \tag{7}$$

is a dimensionless parameter that quantifies the relative deviation [148] of individual time-averaged MSDs about their mean. The characteristics employing the higher moments such as skewness and kurtosis can be implemented additionally to the EB parameter, to characterize finer details of the spread of $\overline{\delta^2}$ trajectories [99].

For SBM considered herein, we numerically solve the stochastic Langevin equation for *massive* particles [109]

$$\frac{d^2x(t)}{dt^2} + \gamma(t)\frac{dx(t)}{dt} = \sqrt{2D(t)}\gamma(t)\eta(t), \qquad (8)$$

driven by the Gaussian noise $\eta(t)$ with zero mean $\langle\eta(t)\rangle = 0$ and unit variance $\langle\eta(t)\eta(t')\rangle = \delta(t - t')$. The friction coefficient is a time dependent function $\gamma(t) = \tau_v^{-1}(t)$, where

$$\tau_v^{-1}(t) = \gamma_0\sqrt{\frac{\mathcal{T}(t)}{\mathcal{T}(0)}} \qquad (9)$$

contains the time dependent temperature $\mathcal{T}(t)$. For instance, for force-free cooling granular gases this dependence is characterized by the law [109]

$$\mathcal{T}(t) = \frac{\mathcal{T}_0}{(1 + t/\tau_0)^{2-2\alpha}}. \qquad (10)$$

For viscoelastic granular gases the exponent is $\alpha = \frac{1}{6}$, while for granular gases with a constant restitution coefficient $\alpha = 0$ [95,112,113]. Correspondingly, the time dependent diffusion coefficient of the particles is

$$D(t) = \frac{D_0}{(1 + t/\tau_0)^{1-\alpha}}, \qquad (11)$$

where the initial values are $\mathcal{T}_0 = \mathcal{T}(0)$ and $D_0 = D(0)$. Putting the Boltzmann constant hereafter to unity ($k_B = 1$) we get the time-local fluctuation-dissipation relation [109]

$$D(t) = \frac{\mathcal{T}(t)}{\gamma(t)m}. \qquad (12)$$

Note that the characteristic scale of the temperature variation τ_0 is much longer than the typical relaxation time in the system

$$\tau_0\gamma_0 \gg 1. \qquad (13)$$

This condition assures the applicability of the initial Langevin equation (8).

The second order Langevin equation (8) is equivalent to two differential equations of the first order for the increments of the particle position $x(t)$ and velocity $v(t)$ [150,151], namely (assuming unit particle mass $m = 1$ from hereon),

$$dv(t) = \sqrt{2D(t)}\gamma(t)\eta(t)\sqrt{dt} - \gamma(t)v(t)dt, \qquad (14)$$

$$dx(t) = v(t)dt. \qquad (15)$$

We discretize this system of equations in $T/\delta t$ steps and use the unit time step in our simulations ($\delta t = 1$). Hence, on time step t_{n+1} the following discrete scheme is solved:

$$v(t_{n+1}) = v(t_n) + \sqrt{2D(t_n)}\gamma(t_n)\eta(t_n)\sqrt{t_{n+1} - t_n} - \gamma(t_n)v(t_n)(t_{n+1} - t_n), \qquad (16)$$

$$x(t_{n+1}) = x(t_n) + v(t_n)(t_{n+1} - t_n). \qquad (17)$$

III. MAIN RESULTS: AGING UDSBM

In this section we present our results for the ensemble- and time-averaged MSDs of UDSBM. We also quantify the amplitude scatter of individual time-averaged MSD trajectories of this process. We first present the analytical results for the UDSBM process and then compare them with computer simulations.

A. MSD

To obtain the ensemble-averaged MSD, we start with the velocity-velocity correlation function, that can be directly obtained via integration of the Langevin equation (8): assuming without loss of generality that $t_2 > t_1$ and applying the same approximations as described in Ref. [109] to evaluate the integrals, we find

$$\langle v(t_1)v(t_2)\rangle \approx D_0\gamma_0\left(1 + \frac{t_1}{\tau_0}\right)^{2\alpha-2}$$
$$\times \exp\left\{\frac{\tau_0\gamma_0}{\alpha}\left[\left(1 + \frac{t_1}{\tau_0}\right)^\alpha - \left(1 + \frac{t_2}{\tau_0}\right)^\alpha\right]\right\}. \qquad (18)$$

Note here that throughout the text the $\approx$ sign has the meaning of approximate equality, the symbol $\sim$ means asymptotically equal, and the sign $\simeq$ indicates asymptotic equality up to a numerical prefactor.

The correlation function (18) is obtained under the condition (13). The ensemble-averaged MSD of diffusing particles can be obtained via the integration of the correlation function (18),

$$\langle x^2(t)\rangle = 2\int_0^t dt_1 \int_{t_1}^t dt_2\langle v(t_1)v(t_2)\rangle. \qquad (19)$$

The reader is referred to our recent study [109] for details on the derivation of $\langle v(t_1)v(t_2)\rangle$ and the MSD for the nonaging UDSBM process. In short, at $t_a = 0$ one gets

$$\langle x^2(t)\rangle \approx 2D_0\left[\frac{\tau_0}{\alpha}\left[\left(1 + \frac{t}{\tau_0}\right)^\alpha - 1\right]\right.$$
$$\left. + \gamma_0^{-1}\left(\exp\left\{-\frac{\tau_0\gamma_0}{\alpha}\left[\left(1 + \frac{t}{\tau_0}\right)^\alpha - 1\right]\right\} - 1\right)\right]. \qquad (20)$$

In the more general situation when the recording of particle position starts after the aging time t_a, the MSD of the aging UDSBM process is described by

$$\langle x_a^2(t)\rangle = 2\int_{t_a}^{t_a+t} dt_1 \int_{t_1}^{t_a+t} dt_2\langle v(t_1)v(t_2)\rangle. \qquad (21)$$

The integration over t_2 can be performed to yield

$$\langle x_a^2(t)\rangle = \frac{2D_0\tau_0\gamma_0}{\alpha}\left(\frac{\alpha}{\tau_0\gamma_0}\right)^{\frac{1}{\alpha}}\int_{t_a}^{t_a+t} dt_1\left(1 + \frac{t_1}{\tau_0}\right)^{2\alpha-2}$$
$$\times \exp\left\{\frac{\tau_0\gamma_0}{\alpha}\left[\left(1 + \frac{t_1}{\tau_0}\right)^\alpha\right]\right\}\left\{\Gamma\left(\frac{1}{\alpha}, \frac{\tau_0\gamma_0}{\alpha}\left[1 + \frac{t_1}{\tau_0}\right]^\alpha\right)\right.$$
$$\left. - \Gamma\left(\frac{1}{\alpha}, \frac{\tau_0\gamma_0}{\alpha}\left[1 + \frac{t + t_a}{\tau_0}\right]^\alpha\right)\right\}, \qquad (22)$$

where $\Gamma(n,x)$ is the incomplete Gamma function [149]. Since throughout this paper we limit ourselves to the regime (13) and the values of the scaling exponents α are not very large (typically, $\alpha \leqslant 2$), the ratio $\tau_0\gamma_0/\alpha$ remains large in the arguments of the Gamma functions. Therefore, for most realistic applications, the expansion of the Gamma functions for large arguments can be performed. The same level of approximations was implemented when obtaining the velocity-velocity correlation function in Eq. (18). After expansion (up to the appropriate order) this procedure yields the following result for the MSD:

$$
\langle x_a^2(t) \rangle \approx \frac{2D_0\tau_0}{\alpha}\left[\left(1+\frac{t+t_a}{\tau_0}\right)^\alpha - \left(1+\frac{t_a}{\tau_0}\right)^\alpha\right]
$$
$$
+ \frac{2D_0}{\gamma_0}\left(\exp\left\{-\frac{\tau_0\gamma_0}{\alpha}\left[\left(1+\frac{t_a+t}{\tau_0}\right)^\alpha\right.\right.\right.
$$
$$
\left.\left.\left.-\left(1+\frac{t_a}{\tau_0}\right)^\alpha\right]\right\}-1\right). \tag{23}
$$

1. Limiting cases

Let us mention here some special cases. If we set $t_a = 0$ in Eq. (23), the MSD of the nonaged UDSBM process (20) is recovered. For $\alpha = 1$, the MSD behaves as that for standard Brownian motion [117], namely,

$$
\langle x_a^2(t) \rangle = \langle x^2(t) \rangle = 2D_0\{t - \gamma_0^{-1}[1 - \exp(-\gamma_0 t)]\}. \tag{24}
$$

This expression and its scaling behaviors are shown in Fig. 1(a).

In the limit of very long observation and long aging times, when $\tau_0 \ll t_a \ll t$, we can neglect the second square bracket term in Eq. (23). The final MSD then coincides with the MSD of nonaging UDSBM at long observation times [109], namely,

$$
\langle x_a^2(t) \rangle \sim \frac{2D_0\tau_0}{\alpha}\left(\frac{t}{\tau_0}\right)^\alpha \simeq t^\alpha. \tag{25}
$$

The most interesting situation emerges when the aging time is the longest time scale in the problem, $\gamma_0^{-1} \ll \tau_0 \ll t_a$ and $t \ll t_a$. For very small values of the argument (arg) of the exponential function in Eq. (23),

$$
\text{arg} = \frac{\tau_0\gamma_0}{\alpha}\left[\left(1+\frac{t_a+t}{\tau_0}\right)^\alpha - \left(1+\frac{t_a}{\tau_0}\right)^\alpha\right] \ll 1, \tag{26}
$$

after expanding Eq. (23) the aging MSD shows the initial ballistic growth regime

$$
\langle x_a^2(t) \rangle \sim D_0\gamma_0\left(\frac{t_a}{\tau_0}\right)^{2\alpha-2}t^2 \simeq t^2. \tag{27}
$$

Conversely, in the limit arg $\gg 1$ expression (23) yields the normal diffusion regime

$$
\langle x_a^2(t) \rangle \sim 2D_0\left(\frac{\tau_0}{t_a}\right)^{1-\alpha}t \simeq t. \tag{28}
$$

This long aging time MSD behavior is equivalent to that of aging SBM considered in Ref. [107] and it features a linear dependence on the diffusion time t. Therefore, *no anomalous diffusion regime at all* is observed for UDSBM when the aging
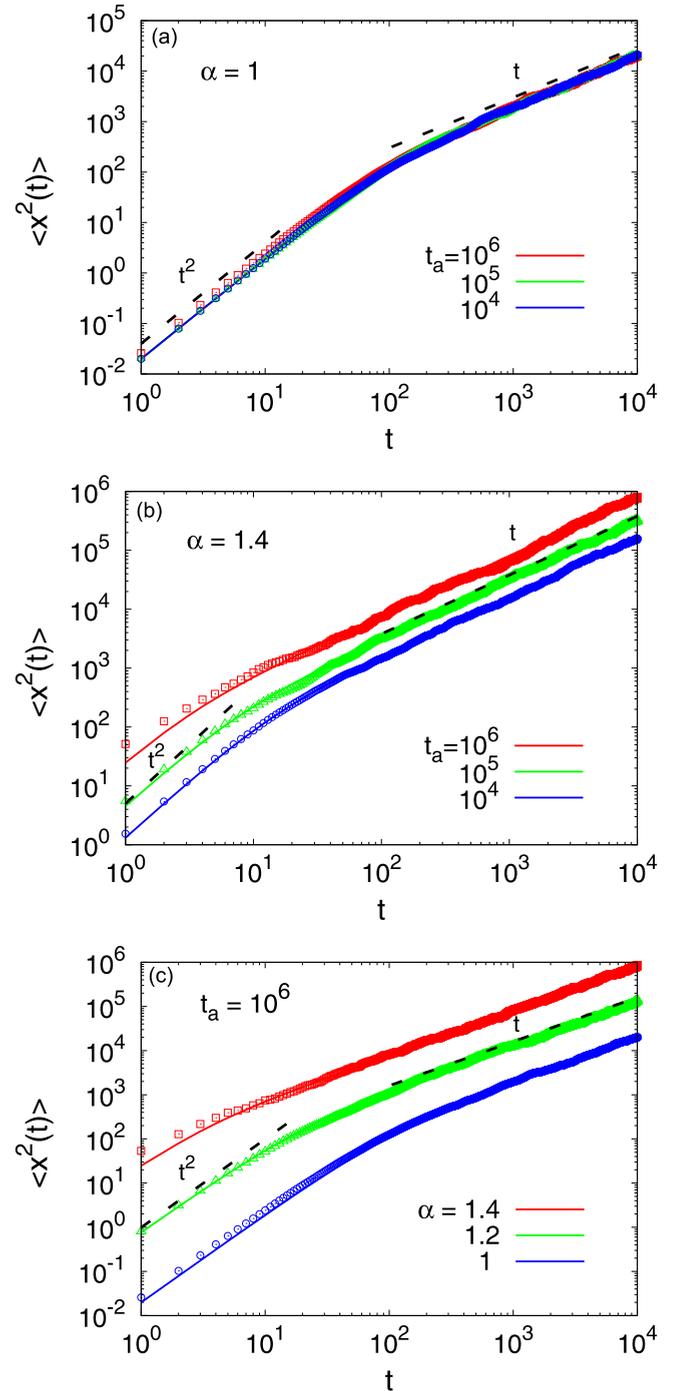
FIG. 1. MSD of the aging UDSBM process: analytical results [solid lines, with the full expression of Eq. (23) and with the asymptotes (27) and (28) shown] and the results of computer simulations (data points), plotted for $\alpha = 1$ (a) and $\alpha = 1.4$ (b) and different aging times t_a. Parameters: $\tau_0 = 100$, $\gamma_0 = 0.02$, $m = 1$, $D_0 = 1$, and the observation time is $T = 10^4$. The initial temperature is $\mathcal{T}_0 = m\gamma_0 D_0 = \gamma_0$. In (a) we have $t_{\min} = 50$, for (b) at $t_a = 10^6, 10^5, 10^4$ we have, respectively, $t_{\min} \approx 1.26, 3.16, 7.93$. (c) Shows the MSD for the case of strong aging $t_a = 10^6 \gg T$ and different α. For superdiffusive UDSBM, the ballistic MSD regime shrinks to shorter times $t \ll 1/\gamma_0$ for larger α values, in accord with the analytical prediction (31). In (c) at $t_a = 10^6$ we have $t_{\min} \approx 1.26, 7.93, 50$ for $\alpha = 1.4, 1.2, 1$, correspondingly.

time is the longest time scale (see Fig. 1). This is a quite remarkable effect of strong aging.

For comparison, note that for the nonaging situation the MSD asymptotes for the initial, intermediate, and long time behaviors of the MSD of UDSBM are, respectively,

$$\langle x^2(t) \rangle \sim D_0 \gamma_0 t^2, \tag{29}$$

$$\langle x^2(t) \rangle \sim 2 D_0 t, \tag{30}$$

and $\langle x^2(t) \rangle \sim D_0 \tau_0 \alpha^{-1} (t/\tau_0)^\alpha$, as derived in Ref. [109].

2. Superdiffusion versus subdiffusion

Different effects in the particle dynamics take place for superdiffusive as compared to subdiffusive scaling exponents, as we show here. For $\alpha > 1$ and at $\gamma_0^{-1} \ll \tau_0 \ll t_a$ (strong aging limit), the condition of arg $\gg 1$ is satisfied for all diffusion times, starting from very short times

$$t_{\min} \sim \gamma_0^{-1} \left(\frac{\tau_0}{t_a} \right)^{\alpha-1} \ll \gamma_0^{-1} \ll \tau_0 \ll t_a. \tag{31}$$

The ballistic regime (27) is observed for $t < t_{\min}$. In other words, almost for the entire observation interval, that is, for $T > t \gtrsim t_{\min}$, *normal* diffusion is observed. Yet, the effective diffusion constant becomes much larger than in the nonaging situation (29), that is,

$$D_{\mathrm{eff}}(t_a) = D_0 \left(\frac{t_a}{\tau_0} \right)^{\alpha-1} \gg D_0, \tag{32}$$

as follows from Eq. (28). The short initial region of ballistic diffusion and the long domain of normal diffusion for the situation $\alpha > 1$ are clearly visible in Figs. 1(b) and 1(c). It is also seen that the region of normal diffusion extends towards shorter times with growing aging times and thus the region of ballistic diffusion shrinks. This trend agrees with the estimate (31) for $t_{\min}$. This is another *a priori* unexpected behavior of aging superdiffusive UDSBM.

For subdiffusive exponents $0 < \alpha < 1$ of the UDSBM process the condition (26) is satisfied for much longer observation times, namely,

$$t < t_{\min} \sim \gamma_0^{-1} \left(\frac{t_a}{\tau_0} \right)^{1-\alpha} \gg \gamma_0^{-1}. \tag{33}$$

Hence, the ballistic diffusion regime (27) extends for times much longer than the relaxation time for normal diffusion γ_0^{-1}. For aging *subdiffusive* UDSBM, the ballistic regime persists much longer than for the *superdiffusive* case. Physically, this is consistent with the intuition that inertia effects are more persistent in time for nonequilibrium UDSBM systems, in which the temperature decreases with time, and thus inertia becomes relatively more relevant. Note that the effective diffusion constant, according to Eq. (27), follows

$$D_{\mathrm{eff}}(t_a) = D_0 \gamma_0 \left(\frac{\tau_0}{t_a} \right)^{2-2\alpha}, \tag{34}$$

and thus for progressive aging becomes much smaller than the basal value $D_0 \gamma_0$ in Eq. (29). As a result, the MSD of aging subdiffusive UDSBM develops slower with time than for the nonaging case (see Fig. 2), despite a longer ballistic regime.
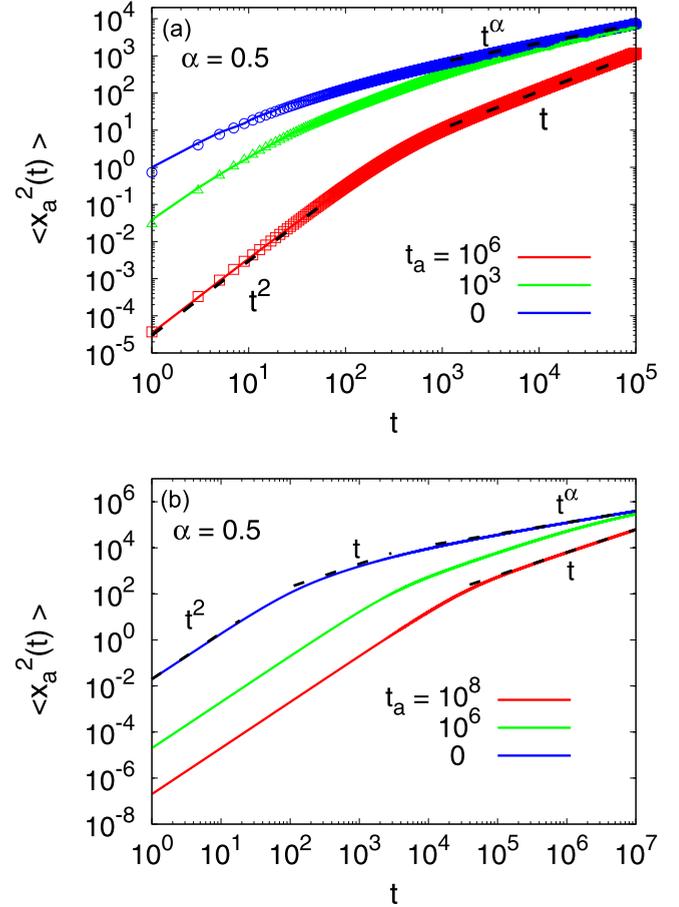
FIG. 2. Delay of the overdamping transition for aging UDSBM. (a) Theoretical (solid lines) and computer simulation (data points) results for the MSD, obtained for $\alpha = 0.5$. The initial ballistic regime is the dashed line following Eq. (27). The intermediate normal diffusion asymptote is the dashed line (28). The trace length is $T = 10^5$ and the aging times t_a are as indicated. Parameters: $D_0 = 1$, $\gamma_0 = 1$, $\tau_0 = 30$. For (a) at $t_a = 10^6, 10^3, 0$ we obtain $t_{\min} \approx 183, 5.77, 1$, respectively. (b) Theoretical results for the MSD, plotted for different aging times and for $\alpha = 0.5$, $D_0 = 1$, $\gamma_0 = 0.02$, $\tau_0 = 10^3$, $T = 10^7$, show three different scaling regimes. Note that the values of τ_0, γ_0, and T in (b) differ from those in (a). For (b), at $t_a = 10^8$, 10^6, and 0 we get $t_{\min} \approx 15,800, 1,580, 50$, respectively. The dashed asymptotes are according to Eqs. (27), (28), and (35).

The temperature in the system at $\alpha < 1$ drops with time [Eq. (10)], and thus the amplitude of stochastic jiggling of the particles gets reduced too. In contrast, for the aging superdiffusive UDSBM process, despite a very short initial ballistic regime, the overall MSD magnitude at a given diffusion time, $\langle x_a^2(t) \rangle$, grows with the aging time [see Fig. 1(b)]. The reason is that the thermal agitation of particles gets more intense with the diffusion time because of growing temperature in the system.

The MSD behavior for aging subdiffusive UDSBM is illustrated in Fig. 2 for two sets of the model parameters. Since the time $t_{\min}$ in Eq. (33) grows with the aging time t_a, the region of ballistic diffusion becomes more extended, as clearly seen when comparing the curves for different t_a values in Fig. 2. The MSD reveals a good agreement of theory and computer simulations, for all values of the model parameters examined.

In Fig. 2, we show the MSD for the trace lengths $T = 10^5$ and 10^7 on Figs. 2(a) and 2(b), respectively. We observe that for longer t_a the region of initial ballistic diffusion and the intermediate regime of normal diffusion are visibly prolonged. For subdiffusive realizations, in the long time limit $t \gg t_a$, the anomalous behavior

$$\langle x_a^2(t) \rangle \sim \frac{2D_0 \tau_0}{\alpha} \left(\frac{t}{\tau_0} \right)^\alpha \simeq t^\alpha \qquad (35)$$

persists, as follows from Eq. (23). In Fig. 2, however, this regime is realized for $t_a = 0$ only because of a relatively short trajectory length T. For the case of superdiffusion in Fig. 1, this anomalous regime is not visible at all because the values of the aging time used are large compared to the trace length T.

B. Time-averaged MSD

1. General expressions

The time-averaged MSD (4) for the aging UDSBM process is defined as [11]

$$\left\langle \overline{\delta_a^2(\Delta)} \right\rangle = \frac{1}{T - \Delta} \int_{t_a}^{T + t_a - \Delta} dt$$
$$\times [\langle x^2(t + \Delta) \rangle - \langle x^2(t) \rangle - 2A(t, \Delta)], \qquad (36)$$

where the last term is computed from the nonaging velocity-velocity correlation function (18) as

$$A(t, \Delta) = \int_0^t dt_1 \int_t^{t+\Delta} dt_2 \langle v(t_1)v(t_2) \rangle. \qquad (37)$$

Following the strategy outlined in Ref. [109], we divide the integral in Eq. (36) formally into two parts, namely,

$$\left\langle \overline{\delta_a^2(\Delta)} \right\rangle = \left\langle \overline{\delta_{0,a}^2(\Delta)} \right\rangle + \langle \Xi_a(\Delta) \rangle. \qquad (38)$$

The first term here corresponds to the time-averaged MSD of the aging SBM process for massless particles [107,108]

$$\left\langle \overline{\delta_{0,a}^2(\Delta)} \right\rangle = \frac{2D_0 \tau_0^2}{\alpha(1 + \alpha)(T - \Delta)}$$
$$\times \left[\left(1 + \frac{T + t_a}{\tau_0} \right)^{\alpha+1} - \left(1 + \frac{t_a + \Delta}{\tau_0} \right)^{\alpha+1} \right.$$
$$\left. - \left(1 + \frac{T + t_a - \Delta}{\tau_0} \right)^{\alpha+1} + \left(1 + \frac{t_a}{\tau_0} \right)^{\alpha+1} \right],$$
$$(39)$$

corresponding to the overdamped limit of the process [107,108]. The second term $\langle \Xi_a(\Delta) \rangle$ is due to the inertial term in the Langevin equation, which is absent in the standard SBM process. Under the condition (13) we obtain the closed form solution

$$\langle \Xi_a(\Delta) \rangle \approx \frac{2D_0}{\gamma_0(T - \Delta)} \int_{t_a}^{T + t_a - \Delta} dt$$
$$\times \left(\exp \left\{ -\frac{\tau_0 \gamma_0}{\alpha} \left[\left(1 + \frac{t + \Delta}{\tau_0} \right)^\alpha \right.\right.\right.$$
$$\left.\left.\left. - \left(1 + \frac{t}{\tau_0} \right)^\alpha \right] \right\} - 1 \right). \qquad (40)$$

The final integration cannot be performed for arbitrary values of α. Below, we consider the important limiting cases.

2. Limiting cases

At $t_a \to 0$ we recover the time-averaged MSD of the nonaging UDSBM process (see Eqs. (42) and (43) in Ref. [109]). For normal diffusion at $\alpha = 1$ from Eqs. (38), (39), and (40) we observe, as expected, no dependence on the aging time:

$$\left\langle \overline{\delta_a^2(\Delta)} \right\rangle = \left\langle x_a^2(\Delta) \right\rangle = \langle x^2(\Delta) \rangle$$
$$= 2D_0 \{ \Delta - \gamma_0^{-1} [1 - \exp(-\gamma_0 \Delta)] \}. \qquad (41)$$

In the most interesting limit of strong aging, when the condition

$$t_a \gg T \gg \{ \Delta, \tau_0 \} \qquad (42)$$

is satisfied, the leading order term in Eq. (39) grows linearly with the lag time,

$$\left\langle \overline{\delta_{0,a}^2(\Delta)} \right\rangle \sim 2D_0 \Delta \left(\frac{t_a}{\tau_0} \right)^{\alpha-1} \simeq \Delta. \qquad (43)$$

In the same limit, Eq. (40) can be represented by

$$\langle \Xi_a(\Delta) \rangle \approx -\frac{2D_0}{\gamma_0} \left\{ 1 - \frac{1}{T - \Delta} \int_{t_a}^{T + t_a - \Delta} dt \right.$$
$$\left. \times \exp \left[-\gamma_0 \Delta \left(\frac{t}{\tau_0} \right)^{\alpha-1} \right] \right\}. \qquad (44)$$

This expression will be used below, for instance, to estimate the time intervals for the initial ballistic behavior of the time-averaged MSD of aging UDSBM. We consider the limit of strong aging in Sec. III B 3, while the limit of short aging times is presented in Sec. III B 4, for the sake of completeness. Note also that for nonaging UDSBM in the intermediate lag time regime $\tau_0 \ll \Delta \ll T$ the leading scaling for the time-averaged MSD is linear, similar to that of the overdamped SBM process [109]

$$\left\langle \overline{\delta_0^2(\Delta)} \right\rangle \sim \frac{2D_0 \Delta}{\alpha} \left(\frac{T}{\tau_0} \right)^{\alpha-1} \simeq \Delta. \qquad (45)$$

3. Superdiffusion versus subdiffusion: Strong aging

We start our analysis with the case of superdiffusion, presented in Fig. 3. As one can see, the argument of the exponential function in Eq. (44) in the limit of strong aging becomes very large already for lag times much shorter than the characteristic relaxation time $1/\gamma_0$. The contribution of the term $\langle \Xi_a(\Delta) \rangle$ to the time-averaged MSD (38) can then be neglected, as compared to the leading Brownian term given by Eq. (43). The initial ballistic regime in the time-averaged MSD in this limit $t_a \gg T$ is then observed only for very short times

$$\Delta \ll 1/\gamma_0,$$

as indeed demonstrated in Fig. 3.

Here, we observe an interesting effect, namely, with increasing lag times the MSD scaling exponent changes from the ballistic value of $\alpha = 2$ to the normal diffusion value $\alpha = 1$ and then back to a higher value of $\alpha = 1.5$. The reader is also
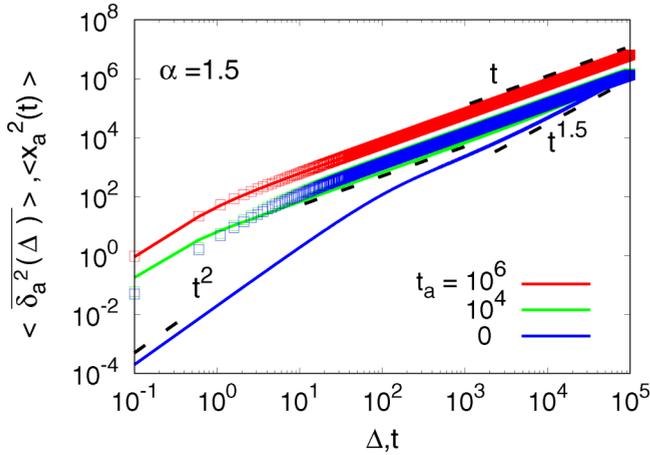
FIG. 3. Analytical results for the MSD (solid lines) and time-averaged MSD (data points) of aging superdiffusive UDSBM at $\alpha = 1.5$. The asymptotes for the initial ballistic, intermediate linear, and long time anomalous behavior are according to Eqs. (27), (28), and (25), respectively. Note that long aging times diminish and eventually remove the weak ergodicity breaking. Parameters: $T = 10^5$, $\tau_0 = 10^3$, and $\gamma_0 = 0.02$. For these parameters, at $t_a = 10^6$, 10^4, and 0 the ballistic regime is expected to range in $t < t_{\min} \approx 1.58$, 15.8, and 50, respectively. Also note the almost fully superimposing time-averaged MSD data points at aging times $t_a = 0$ and $t_a = 10^4$.

referred to Fig. 1 of Ref. [109] for the behavior of nonaging UDSBM. With growing aging time, the initial ballistic regime of the MSD shortens severely [compare the curves and the values of $t_{\min}(t_a)$ in the caption of Fig. 3]. Also, it is important to note that for longer aging times, the aging superdiffusive UDSBM process becomes more ergodic, as one can judge from Fig. 3. In this limit, the ensemble- and time-averaged MSD nearly coincide in the range of diffusion times we examined.

In the case of subdiffusion (Fig. 4), we expand the exponential function in Eq. (40) or (44) up to the second order in Δ and then integrate. The terms linear in the lag time from the main contribution (39) and from the additional term (44) vanish, while the second order in Δ produces for the time-averaged MSD the initial ballistic regime

$$\left\langle \overline{\delta_a^2(\Delta)} \right\rangle \sim D_0 \gamma_0 \left(\frac{t_a}{\tau_0} \right)^{2\alpha - 2} \Delta^2 \simeq \Delta^2. \tag{46}$$

This regime extends up to lag times

$$\Delta < \Delta_{\min} \sim (t_a/\tau_0)^{1-\alpha}/\gamma_0, \tag{47}$$

that is much longer than the characteristic time $1/\gamma_0$ as t_a/τ_0 is a large parameter. Therefore, comparing Eq. (27) for the MSD and Eq. (46) for the time-averaged MSD, one can conclude that the initial ballistic behavior of strongly aging subdiffusive UDSBM is nearly ergodic. This important effect is illustrated in Fig. 5(b), which also shows how the ergodicity of aging UDSBM is recovered in the limit of long aging times.

The short lag time asymptote (46) and the full expression given by Eqs. (39) and (40) are in a good agreement with the results of our numerical modeling of the Langevin equation (see Fig. 4). In the regime of strong aging when $t_a \gg T$, for strongly subdiffusive UDSBM ($\alpha = \frac{1}{6}$) the quadratic scaling
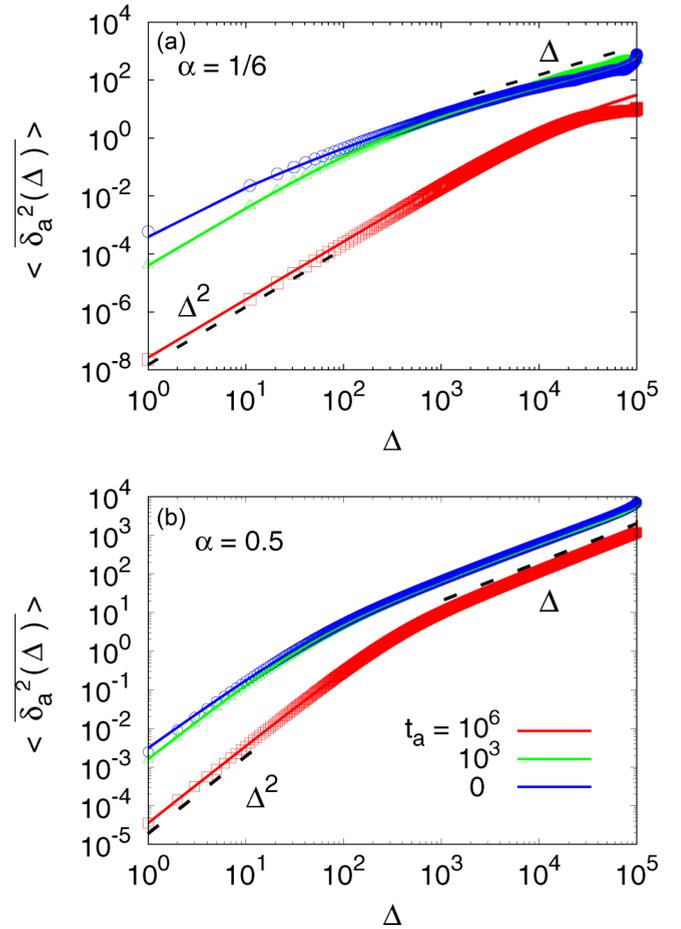
FIG. 4. Theoretical [solid curves, Eqs. (39) and (40)] and computer simulation results (data points) for the time-averaged MSD of aging subdiffusive UDSBM processes. The asymptotes shown as the dashed lines are according to Eqs. (46) and Eqs. (43) and (45) for short and intermediate lag times, respectively. The findings are plotted for $\alpha = \frac{1}{6}$ (a) and $\alpha = \frac{1}{2}$ (b), with $T = 10^5$, $\tau_0 = 10^2$, and $\gamma_0 = 0.1$.

of $\left\langle \overline{\delta_a^2(\Delta)} \right\rangle$ with the lag time extends up to the entire observation period [see Fig. 4(a)]. This is another *a priori* surprising feature, rendering a purely overdamped description invalid in this regime of diffusion times.

The effects of varying aging time for the small value of $\alpha = \frac{1}{6}$, relevant to the behavior of granular gases [95,109], can be seen in Fig. 6 for rather long traces with $T = 10^7$. When the aging time is shorter than the observation time and the relation $T \gg \Delta \gg \tau_0$ is satisfied, the time-averaged MSD has an extended intermediate linear scaling regime, in accord with the analytical prediction (45). This regime disappears in the limit of strong aging by virtue of the fact that the initial ballistic regime for small α values extends to much longer times, in accord with Eq. (47) [see also the curve for $t_a = 10^6$ in Fig. 4(a)]. This intermediate Fickean diffusion regime exists also for nonaging UDSBM [109].

4. Superdiffusion versus subdiffusion: Weak aging

When the lag time Δ is the shortest time scale, we expand the contribution to the time-averaged MSD $\left\langle \overline{\delta_{0,a}^2(\Delta)} \right\rangle$ in
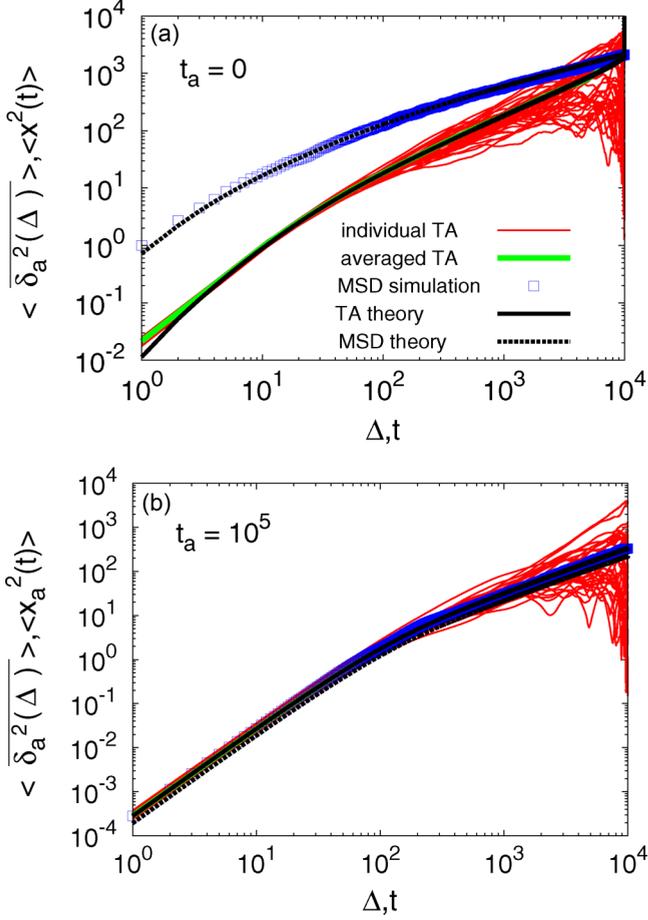
FIG. 5. MSD (blue points and dashed lines) and time-averaged MSD (green lines and solid black line) for the aging subdiffusive UDSBM processes, for $\alpha = \frac{1}{2}$ and two different aging times t_a as indicated in (a) and (b). The analytical expressions for the MSD and time-averaged MSD are given by Eqs. (23) and (38), respectively. The red curves represent individual time-averaged MSD realizations. Other parameters are the same as in Fig. 2(a).
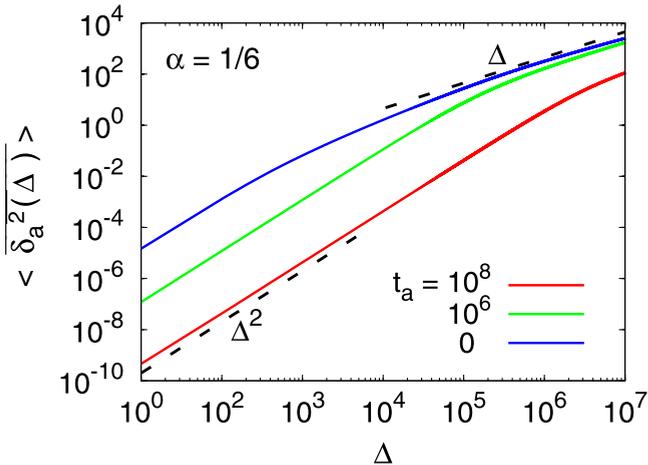
FIG. 6. Analytical results for the time-averaged MSD of aging UDSBM, plotted for $\alpha = \frac{1}{6}$ and varying aging times. The asymptotes are according to Eqs. (46) and (45). Parameters: $T = 10^7$, $\tau_0 = 10^3$, and $\gamma_0 = 0.02$.

Eq. (39) as well as the integrand of $\langle \Xi_a(\Delta) \rangle$ in Eq. (40) for short lag times up to the second order. Taking the integral in Eq. (40) and summing the two terms, we find that the contributions linear in Δ cancel and the leading order is quadratic in Δ. This approximate expression for $\langle \overline{\delta_a^2(\Delta)} \rangle$ at the conditions of weak aging $t_a \ll T$ and in the physically relevant limit of $\tau_0/T \ll 1$ for $0 < \alpha < \frac{1}{2}$ has the form

$$\left\langle \overline{\delta_a^2(\Delta)} \right\rangle \sim \frac{D_0 \gamma_0 \tau_0}{(1-2\alpha)T} \Delta^2, \tag{48}$$

while at $\alpha > \frac{1}{2}$ the leading order is

$$\left\langle \overline{\delta_a^2(\Delta)} \right\rangle \sim \frac{D_0 \gamma_0}{(2\alpha - 1)} \left(\frac{T}{\tau_0} \right)^{2\alpha - 2} \Delta^2. \tag{49}$$

At $\alpha = 1$ this approximate procedure yields

$$\left\langle \overline{\delta_a^2(\Delta)} \right\rangle \sim D_0 \gamma_0 \Delta^2, \tag{50}$$

as follows also from Eq. (41). The critical value of $\alpha = \frac{1}{2}$ demarcates the boundary for different scalings of the $\langle \overline{\delta_a^2(\Delta)} \rangle$ prefactors with the trace length T in the short lag time limits [Eqs. (48) and (49)]. At $\alpha = \frac{1}{2}$ the prefactor becomes a logarithmic rather than a power-law function of the trace length, namely,

$$\left\langle \overline{\delta_a^2(\Delta)} \right\rangle \sim \frac{D_0 \tau_0 \gamma_0}{T} \ln\left(1 + \frac{T}{\tau_0} \right) \Delta^2. \tag{51}$$

5. Time-averaged MSD enhancement or suppression function

Let us now consider the degree of enhancement or suppression of the time-averaged MSD due to the presence of aging [66–68] in the UDSBM process. It is quantified by the ratio of the aging versus nonaging time-averaged MSD magnitudes

$$\Lambda_\alpha(t_a, \Delta) = \frac{\left\langle \overline{\delta_a^2(\Delta)} \right\rangle}{\left\langle \overline{\delta^2(\Delta)} \right\rangle}. \tag{52}$$

Using the relations (46), (48), (49), and (51) for short lag times (corresponding to the ballistic regime), long particle trajectories $\{\Delta, \tau_0\} \ll T$, and strong aging $t_a \gg T$ one gets the following asymptotic form:

$$\Lambda_\alpha(t_a) \sim \begin{cases} (1-2\alpha) \frac{T}{\tau_0} \left(\frac{t_a}{\tau_0} \right)^{2\alpha-2}, & \alpha < 1/2 \\ \frac{T/\tau_0}{\ln(1+T/\tau_0)} \left(\frac{t_a}{\tau_0} \right)^{2\alpha-2}, & \alpha = 1/2 \\ (2\alpha - 1) \left(\frac{t_a}{T} \right)^{2\alpha-2}, & \alpha > 1/2. \end{cases} \tag{53}$$

In this limit, the quadratic dependence of Λ_α on the lag time Δ in time-averaged MSDs cancels out in (53) and the universal power-law scaling (in the leading order) is

$$\Lambda_\alpha(t_a) \simeq t_a^{2\alpha-2}. \tag{54}$$

Note that for the standard overdamped SBM process the suppression (enhancement) function Λ_α for subdiffusive (superdiffusive) realizations of the exponent α is [85,107]

$$\Lambda_\alpha(t_a) \approx \left(1 + \frac{t_a}{T} \right)^\alpha - \left(\frac{t_a}{T} \right)^\alpha. \tag{55}$$
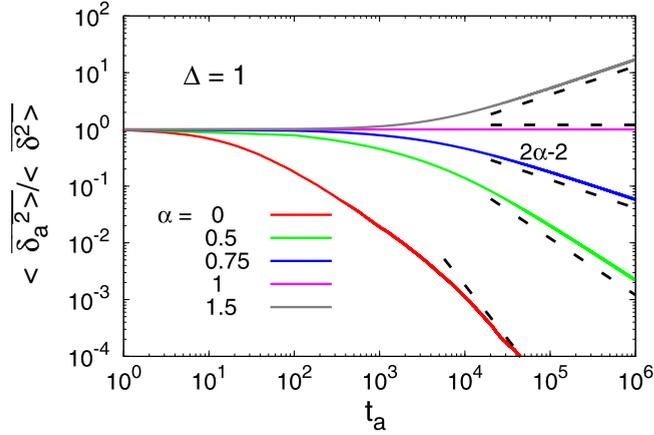
FIG. 7. Ratio of the aging versus nonaging time-averaged MSDs of UDSBM, $\Lambda_\alpha(t_a)$, as obtained from our computer simulations, plotted as a function of the aging time t_a for $\Delta = 1$ and different values of the scaling exponents. Parameters: $T = 10^4$, $\tau_0 = 30$, $N = 10^3$. The analytical asymptotes in the limit of long aging times (53) are shown by the dashed lines.

This power-law function is similar to that observed for aging continuous time random walks [66–68] and aging heterogeneous diffusion processes [83].

For aging superdiffusive UDSBM processes, as predicted by Eq. (53) at $\alpha > 1$, the magnitude of the time-averaged MSD gets enhanced with the aging time, while for subdiffusive UDSBMs realized at $\alpha < 1$ the time-averaged MSD gets

suppressed with increasing t_a. The analytical estimate (53) is in good agreement with our computer simulations of aging UDSBM, as presented in Fig. 7 for systematically varied scaling exponent α. We mention that the smaller the exponent α, the more pronounced is the decrease of the time-averaged MSD with the aging time t_a, while for $\alpha > 1$ the enhancement of the time-averaged MSD is observed, in accord with Eq. (54). In Fig. 5, for a special value of $\alpha = \frac{1}{2}$ we also observe that the time-averaged MSD gets reduced for longer aging times. Finally, note a different dependence of $\Lambda_\alpha(t_a)$ in Eq. (53) on the length of the particle trajectory T for subdiffusive versus superdiffusive UDSBM processes, as well as for the critical value of $\alpha = \frac{1}{2}$.

C. Scatter of time-averaged MSDs and ergodicity breaking parameter

For a finite trajectory length, all stochastic processes exhibit trajectory-to-trajectory fluctuations. These lead to fluctuating apparent mobilities of the particles. Figure 5 illustrates the amplitude scatter of individual time-averaged MSD trajectories of both aging and nonaging UDSBM processes. It appears to be quite narrow and thus the process is fairly reproducible. In particular, the amplitude spread of the $\overline{\delta^2}$ traces changes only moderately with the aging time. At short lag times Δ the spread is rather small, similar to that for the Brownian motion with the same trace length T [11].

Figure 8 shows the amplitude scatter of individual time-averaged MSD traces, $\phi(\xi)$, for both the aging and nonaging
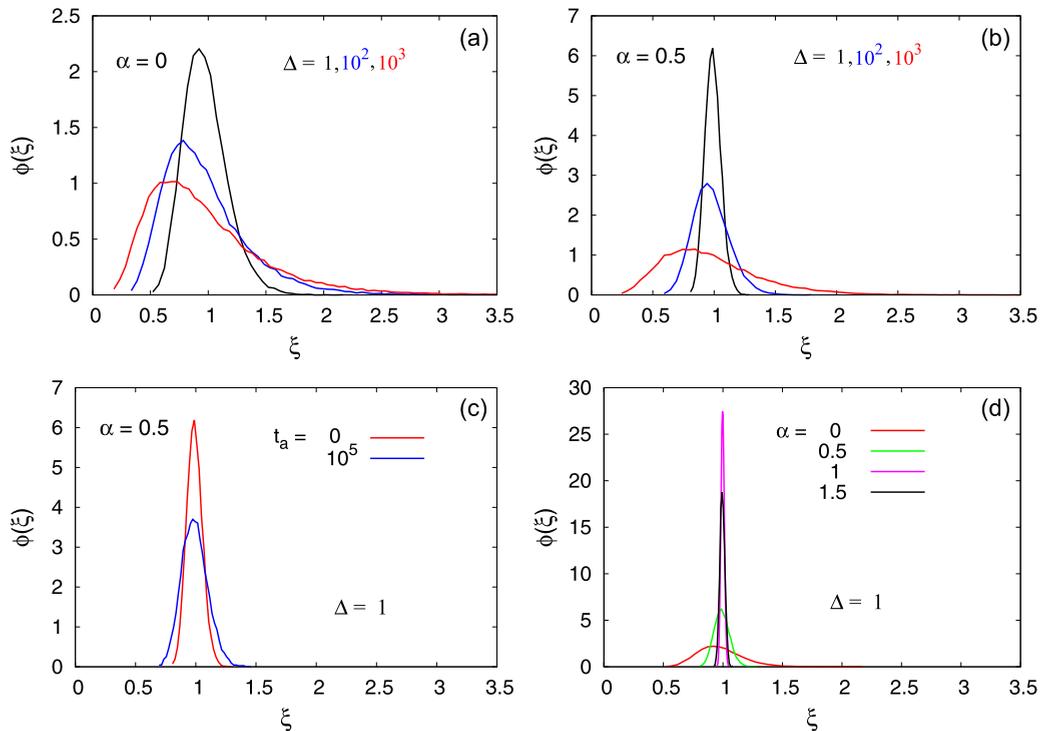
FIG. 8. (a), (b) Distribution $\phi(\xi)$ of the relative amplitude of the time-averaged MSD for nonaging UDSBM at $\alpha = \frac{1}{2}$ and ultraslow UDSBM, computed for different lag times, as indicated in the panels. For longer lag times, the distribution gets progressively wider and becomes asymmetric. (c) Comparison between $\phi(\xi)$ for aging and nonaging UDSBM processes for $\alpha = 0.5$ and lag time $\Delta = 1$. In the strong aging regime, the distribution becomes slightly wider. (d) Distributions $\phi(\xi)$ for the nonaging UDSBM process for different α exponents, as indicated in the plot, and for $\Delta = 1$. Parameters for all the plots: $T = 10^4$ and $N = 10^4$.
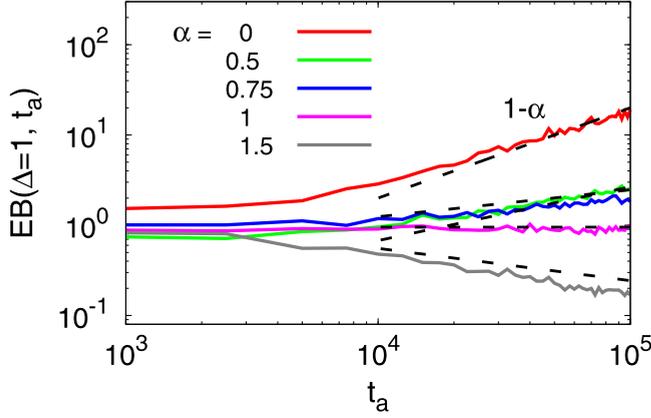
FIG. 9. EB parameter obtained from computer simulations versus the aging time t_a for the aging UDSBM process, computed for traces with $T = 10^4$ steps and averaged over $N = 10^3$ trajectories, for different α values (as denoted in the plot) and $\Delta = 1$. The black dashed lines show the phenomenological strong aging scaling relation (56). The parameters used here are $T = 10^4$, $\tau_0 = 30$, $\tau_v = 1$, and $D_0 = 1$.

UDSBM processes, for a set of values of the diffusion exponent α, lag time Δ, and aging time t_a. We first start with UDSBM in the absence of aging, complementing the results of Ref. [109]. As follows from Figs. 8(a) and 8(b) evaluated at $t_a = 0$, larger values of Δ lead to more asymmetric, noncentered $\phi(\xi)$ distributions. Comparing $\phi(\xi)$ for nonaging ultraslow ($\alpha = 0$) and subdiffusive ($\alpha = \frac{1}{2}$) UDSBM [see Figs. 8(a) and 8(b)], we clearly see a broader spread of time-averaged MSD realizations for $\alpha = 0$ situation.

Systematically larger values of the EB parameter found in simulations of aging UDSBM at $\alpha = 0$, as demonstrated in Fig. 9, are in line with this larger width of $\phi(\xi)$ distributions for the ultraslow UDSBM process (see Sec. IV). In contrast, for superdiffusive realizations the amplitude spread of the time-averaged MSD traces and the magnitudes of the corresponding ergodicity breaking parameters EB are smaller (compare the curves for different α values in Fig. 9). Note that this behavior is quite different from the aging effects for the canonical SBM process. Namely, for the latter in the limit of strong aging $t_a \gg T$ the dependence of EB on the aging time t_a scales out from the final result. In the strong aging limit and for short lag times $\Delta/T \ll 1$ the system approaches the ergodic behavior, with $\mathrm{EB}_{\mathrm{SBM}}(t_a, \Delta) \to \mathrm{EB}(\Delta)_{\mathrm{BM}} = 4\Delta/(3T)$, independent on aging time and α. The reader is referred to Eqs. (44) and (45) and Figs. 5 and 6 in Ref. [108]. The $\mathrm{EB}(t_a)$ dependence for UDSBM processes we detect in the strong aging limit in Fig. 9 is valid in the ballistic regime of the corresponding time-averaged MSD.

For fixed Δ and α values, the presence of aging in the system makes the distributions of the time-averaged MSDs slightly wider [see Fig. 8(c)]. According to Fig. 8(d), showing the results for nonaging UDSBM, by increasing the scaling exponent α up to unity the distributions $\phi(\xi)$ become narrower. For more superdiffusive α values, however, the distribution $\phi(\xi)$ becomes slightly broader again. This effect is similar to the dependence of the EB parameter for the standard SBM process as a function of α (see the description and Fig. 3(a) in Ref. [108]).

A fairly reproducible behavior of time-averaged MSDs, that is, narrow $\phi(\xi)$ distributions observed here, is similar to that of otherwise ergodic fractional Brownian motion and fractional Langevin equation motion [98,118,152]. Note that for these processes the effects of transient aging and weak ergodicity breaking were also studied [119,153,154]. This reproducibility of $\overline{\delta^2}$ for aging UDSBM is in strong contrast, for instance, to continuous time random walks in which time averages of physical observables remain random quantities, even in the limit $T \to \infty$ [11,146].

A commonly used measure of these amplitude fluctuations of $\overline{\delta^2}$ trajectories for UDSBM and other anomalous diffusion processes is the ergodicity breaking parameter, EB [Eq. (6)] [11]. In Fig. 9, we present the variation of EB for aging UDSBM with the aging time t_a, as obtained from our computer simulations. Performing a fitting to data points, we find that for strong aging the following phenomenological scaling is valid:

$$\mathrm{EB}(t_a) \simeq t_a^{1-\alpha}. \tag{56}$$

Therefore, with increasing aging time the EB parameter, for the same value of the lag time, decreases for superdiffusive and grows for subdiffusive aging UDSBM (Fig. 9). The physical explanation is that for subdiffusive cases, the typical rate for jump events of the particle is perpetually decreasing, and along with it the variance of interjump intervals. Thus, the spread between individual trajectories is expected to increase with the aging time. The opposite, a focusing of the interjump intervals, occurs for superdiffusive systems. Note that the full analytical evaluation for the dependence of the EB parameter on the aging time and the scaling exponent for UDSBM is a nontrivial and quite complicated mathematical task, surely beyond the scope of this study. Note that even for the standard SBM process, with a simple particle position correlation function $\langle x(t_1)x(t_2)\rangle$, a nontrivial behavior was revealed for the $\mathrm{EB}(t_a, \Delta)$ dependence in our recent investigation (see Ref. [108]). For the UDSBM processes, the problem of computing the fourth moment of the time-averaged MSD is expected to be even harder than for SBM and thus deserves separate attention.

We note here that the number of traces needed to reach a satisfactory statistics for the EB parameter, containing the fourth moment of the time-averaged MSDs, is typically considerably larger than that required for the convergence of $\langle \overline{\delta_a^2(\Delta)} \rangle$ [108].

The dependence of the EB parameter on the trajectory length T is presented in Fig. 10, for both nonaging and aging UDSBM. In the absence of aging, as shown in Fig. 10(a), the EB parameter in the limit of long trajectories varies as

$$\mathrm{EB}_{\mathrm{nonaging}}(T) \simeq 1/T^\alpha. \tag{57}$$

Note that this scaling for UDSBM at short lag times and thus in the ballistic regime of the time-averaged MSD, as those shown in Fig. 10(a), is different from that for the standard SBM. For the latter, the dependence is $\mathrm{EB}(T) \simeq 1/T^{2\alpha}$ for $0 < \alpha < \frac{1}{2}$ and $\mathrm{EB}(T) \simeq 1/T$ for $\alpha > \frac{1}{2}$ [108]. However, in the limit of strong aging, the decay of EB is inversely proportional with the trace length T:

$$\mathrm{EB}_{\mathrm{aging}}(T) \simeq 1/T, \tag{58}$$
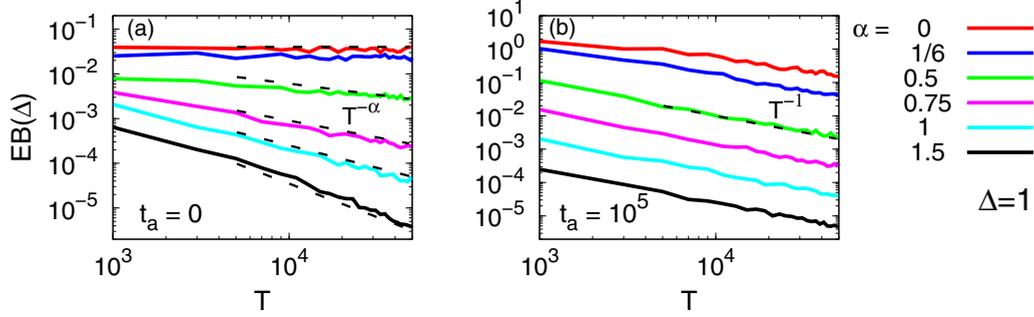
FIG. 10. Ergodicity breaking parameter variation with the trace length T, computed for different scaling exponents α in the absence of aging (a) and for rather strong aging (b), after averaging over $N = 10^3$ trajectories. The value of the lag time is $\Delta = 1$ for both panels so that $\Delta/T \ll 1$. The asymptotes shown in (a) and (b) are Eqs. (57) and (58), in the limit of short and long aging times, respectively.

[see Fig. 10(b)], shown again for a short lag time $\Delta = 1$. The same scaling relation of EB is observed also for longer lag times (not shown). Note that this inverse proportionality of the EB parameter with the trace length is typical for a number of other anomalous diffusion processes [11].

IV. MAIN RESULTS: AGING ULTRASLOW UDSBM

Let us now consider inertial effects for the aging UDSBM process at $\alpha = 0$. The motion of massive particles in this case is governed by the underdamped Langevin equation [109]

$$m\frac{d^2x(t)}{dt^2} + \frac{\gamma_0}{(1+t/\tau_0)}\frac{dx(t)}{dt} = \sqrt{\frac{2D_0}{1+t/\tau_0}}\frac{\gamma_0\eta(t)}{(1+t/\tau_0)}. \quad (59)$$

A. MSD

We straightforwardly obtain the velocity autocorrelation and find in the limit $\tau_0\gamma_0 \gg 1$ that

$$\langle v(t_1)v(t_2)\rangle \approx \frac{\mathcal{T}(0)}{m}\left(\frac{1+t_1/\tau_0}{1+t_2/\tau_0}\right)^{\tau_0\gamma_0}\frac{1}{(1+t_1/\tau_0)^2}. \quad (60)$$

This expression can be directly obtained from Eq. (18) by putting $\alpha \to 0$. After some simplifications, the MSD of aging ultraslow UDSBM acquires both a logarithmic and power-law function of the diffusion time t:

$$\langle x_a^2(t)\rangle \sim 2D_0\tau_0 \ln\left(1 + \frac{t}{t_a + \tau_0}\right)$$
$$+ \frac{2D_0}{\gamma_0}\left[\left(1 + \frac{t}{t_a + \tau_0}\right)^{-\tau_0\gamma_0} - 1\right]. \quad (61)$$

We restrict the analysis of this equation to the most interesting situation of strong aging,

$$t_a \gg \{t,\tau_0\}. \quad (62)$$

In this limit, Eq. (61) can be approximated by

$$\langle x_a^2(t)\rangle \sim 2D_0\tau_0\frac{t}{t_a} - \frac{2D_0}{\gamma_0}\left(1 - \exp\left[-\frac{t}{t_a}\tau_0\gamma_0\right]\right). \quad (63)$$

In the argument of the exponent we thus observe a product of a large parameter $\tau_0\gamma_0$ and a small parameter t/t_a. Therefore, for the range of diffusion times up to

$$t < t_{\min} \sim t_a/(\tau_0\gamma_0), \quad (64)$$

the leading order expansion of Eq. (63), the MSD of aging ultraslow UDSBM, similarly to the MSD for the nonaging UDSBM process [109], shows the ballistic regime

$$\langle x_a^2(t)\rangle \sim \frac{D_0\tau_0^2\gamma_0}{t_a^2}t^2 \simeq t^2. \quad (65)$$

Figure 11(a) shows that this regime extends to times much longer than the relaxation time $1/\gamma_0$ for standard diffusion [117] of massive Brownian particles.

For the subsequent diffusion regime satisfying the condition $t > t_{\min} \sim t_a/(\tau_0\gamma_0)$, the first term in Eq. (63) dominates, yielding the linear MSD growth with time

$$\langle x_a^2(t)\rangle \sim 2D_0\tau_0\frac{t}{t_a} \simeq t. \quad (66)$$

Similarly to nonaging UDSBM [109], for long observation times $t \gg \{t_a,\tau_0\}$ the MSD of the aging ultraslow UDSBM process demonstrates (as expected) a logarithmic dependence on the diffusion time

$$\langle x_a^2(t)\rangle \sim 2D_0\tau_0 \ln\left(\frac{t}{t_a}\right). \quad (67)$$

B. Time-averaged MSD

The aging time-averaged MSD of the ultraslow UDSBM process acquires a form similar to Eq. (38), namely, a combination of two terms. Here, the main contribution to the time-averaged MSD coincides with that of the nonaging ultraslow UDSBM process in the limit (13), that is (see Eq. (61) in Ref. [109]),

$$\left\langle\overline{\delta_{0,a}^2(\Delta)}\right\rangle \approx \frac{2D_0\tau_0}{T-\Delta}\int_{t_a}^{T+t_a-\Delta} dt' \ln\left(1 + \frac{\Delta}{\tau_0+t'}\right)$$
$$= \frac{2D_0\tau_0}{T-\Delta}\left[(T+t_a+\tau_0)\ln\left(1 + \frac{T+t_a}{\tau_0}\right)\right.$$
$$-(t_a+\tau_0+\Delta)\ln\left(1 + \frac{t_a+\Delta}{\tau_0}\right)$$
$$- (T+t_a+\tau_0-\Delta)\ln\left(1 + \frac{T+t_a-\Delta}{\tau_0}\right)$$
$$\left.+ (t_a+\tau_0)\ln\left(1 + \frac{t_a}{\tau_0}\right)\right]. \quad (68)$$
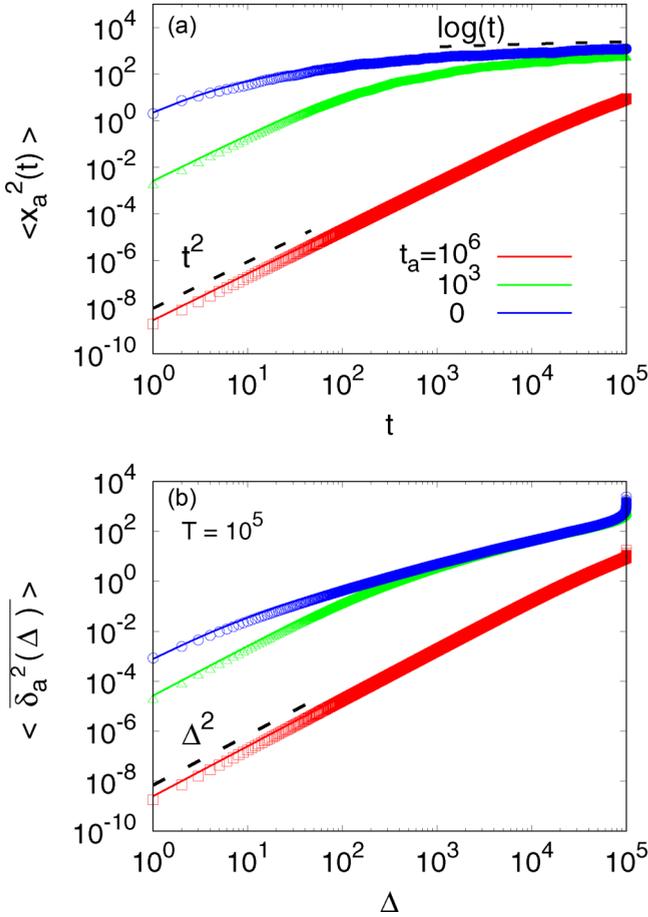
FIG. 11. MSD (a) and time-averaged MSD (b) as obtained from computer simulations (data points) and theoretically [solid lines; Eq. (61) for the MSD and Eqs. (68) and (69) for the time-averaged MSD] for the aging ultraslow UDSBM process at $\alpha = 0$. The short time ballistic asymptote and the long time logarithmic behavior of the MSD are shown as dashed lines, plotted according to Eqs. (65) and (67), correspondingly. The ballistic asymptotes for the time-averaged MSD are the dashed lines [Eq. (70)]. The values of the aging time t_a are as indicated in the plots. Other parameters are $D_0 = 1$, $\gamma_0 = 1$, and $\tau_0 = 30$.

The second contribution to the time-averaged MSD describes the inertial term in the original Langevin equation (59), namely,

$$\langle \Xi_a(\Delta) \rangle \approx \frac{2D_0}{\gamma_0(T - \Delta)} \int_{t_a}^{T+t_a-\Delta} dt'$$
$$\times \left[\left(1 + \frac{\Delta}{t' + \tau_0} \right)^{-\tau_0 \gamma_0} - 1 \right]. \quad (69)$$

Using for Eq. (69) the exponential representation analogous to that used for Eq. (44) in the limit of long aging times, $t_a \gg \{T, \Delta\}$, we get the initial ballistic regime of the time-averaged MSD:

$$\left\langle \overline{\delta_a^2(\Delta)} \right\rangle \sim D_0 \gamma_0 \left(\frac{\tau_0}{t_a} \right)^2 \Delta^2 \simeq \Delta^2. \quad (70)$$

Note that this relation can be also directly obtained from Eq. (46) by setting $\alpha \to 0$. The ballistic regime (70) extends

up to lag times satisfying the condition

$$\Delta < \Delta_{\min} \sim t_a / (\tau_0 \gamma_0), \quad (71)$$

that is much longer that the relaxation time $1/\gamma_0$. We remind the reader that the latter defines the time scale of the ballistic regime for ordinary Brownian motion [Eq. (29)]. Note that the effective diffusion constant for the aging ultraslow UDSBM process,

$$D_{\mathrm{eff}}(t_a) = D_0 \gamma_0 \left(\frac{\tau_0}{t_a} \right)^2, \quad (72)$$

in this limit of strong aging becomes much smaller than for normal Brownian motion, $D_0 \gamma_0$. Figure 11 demonstrates a good agreement between our computer simulations of the underdamped equation (59) for the aging ultraslow UDSBM process and the theoretical results, for both the MSD and the time-averaged MSD. Finally, the scatter of time-averaged MSDs for nonaging ultraslow UDSBM is illustrated in Fig. 8(a).

V. DISCUSSION AND CONCLUSIONS

In this study, we rationalized the effects of aging on the ensemble-averaged MSD, the time-averaged MSD, and the ergodic properties of the underdamped SBM process (UDSBM). We explicitly considered the effects of a *finite particle mass* on the magnitude and duration of the short time ballistic regime, both for the MSD and the time-averaged MSD. The thorough investigation of the effects of aging on the UDSBM process complements and completes our recent study [109] of nonaging UDSBM. Our findings support the idea that in nonstationary diffusive systems the presence of aging can drastically alter the particle dynamics, at short, intermediate, and long time limits. Additionally, the current study extends the range of scaling behaviors predicted for the nonaging UDSBM processes [109].

The existence and unexpectedly long persistence of the short time ballistic regime for nonaging UDSBM was first predicted in Ref. [109]. In the presence of aging, however, the duration of this regime depends on the anomalous exponent as well as the aging time. For subdiffusive exponents, both the MSD and the time-averaged MSD of aging UDSBM show a ballistic behavior for times considerably longer than that for ordinary Brownian motion, $1/\gamma_0$, namely for $(t, \Delta) < (t, \Delta)_{\min} \sim \gamma_0^{-1} (\frac{t_a}{\tau_0})^{1-\alpha}$ [Eqs. (33) and (47)]. At later times, a transition to normal diffusion is observed for the aging and nonaging UDSBM processes. In contrast, for superdiffusive exponents $\alpha > 1$ the normal diffusive regime dominates the MSD in the intermediate and long time regime, while the ballistic regime exists only at very short times, $t < t_{\min} \sim \gamma_0^{-1} (\frac{\tau_0}{t_a})^{\alpha-1}$ [Eq. (31)]. Our analytical results are supported by the findings of extensive computer simulations of the stochastic Langevin equation for massive particles in a medium with time varying diffusivity.

We characterized the behavior of the system both for subdiffusive and superdiffusive scaling exponents α, as well as for the limiting value of $\alpha = 0$. The latter gives rise to ultraslow UDSBM, with a characteristic combined logarithmic and power-law time dependence of the averaged particle

displacement. The ballistic regime of aging ultraslow UDSBM extends up to $(t,\Delta)_{\min} \sim t_a/(\tau_0\gamma_0)$, both for the MSD and time-averaged MSD [Eqs. (64) and (71)]. Particularly for subdiffusive UDSBM processes we demonstrated that in the limit of long aging times, the overdamping approximation fails entirely. Instead, the initial ballistic regime expected for massive particles extends for large t_a values up to the entire trace length, i.e., times much longer than typical relaxation time $1/\gamma_0$.

Aging is shown to reduce the magnitude of the time-averaged MSD for the case of subdiffusion and to increase it in the superdiffusion case, in accord with the universal scaling $\Lambda_\alpha \simeq t_a^{2\alpha-2}$ at strong aging [Eq. (54)]. We also showed that for long aging times in the ballistic regime, the MSD converges to the time-averaged MSD and thus ergodicity is restored for the aging UDSBM processes, both for subdiffusive and superdiffusive situations. We also analyzed the nonergodicity of aging UDSBM based on the ergodicity breaking parameter, EB. Based on computer simulations, we demonstrated that

the presence of aging changes the decay of EB. Specifically, for long observation times the EB of the UDSBM process in the limit of strong aging decays as $EB \simeq T^{-1}$ [Eq. (58)], contrasting the asymptotic scaling $EB \simeq T^{-\alpha}$ for nonaging UDSBM [Eq (57)].

The applications of our results to real physical systems include the behavior and dynamics of particles in granular gases, with the power-law decrease of the medium temperature [95,109,112]. It will be interesting to compare our results to more detailed simulations of these systems. The development of underdamped particle dynamics and approaches for other anomalous diffusion processes is also of great interest. For instance, the limits of applicability of the commonly used overdamping approximation for continuous time random walks, known to be connected to SBM in a mean field sense [106], would be intriguing to unravel in the future. Finally, the definition of applicability criteria of overdamped approximation for other anomalous diffusion processes is of vital importance.

[1] J. W. Haus and K. W. Kehr, Phys. Rep. **150**, 263 (1987).

[2] J.-P. Bouchaud and A. Georges, Phys. Rep. **195**, 127 (1990).

[3] S. Havlin and D. Ben-Avraham, Adv. Phys. **51**, 187 (2002).

[4] R. Metzler and J. Klafter, Phys. Rep. **339**, 1 (2000).

[5] S. Burov, J.-H. Jeon, R. Metzler, and E. Barkai, Phys. Chem. Chem. Phys. **13**, 1800 (2011).

[6] E. Barkai, Y. Garini, and R. Metzler, Phys. Today **65**(8), 29 (2012).

[7] I. M. Sokolov, Soft Matter **8**, 9043 (2012).

[8] M. J. Saxton, Biophys. J. **103**, 2411 (2012).

[9] F. Höfling and T. Franosch, Rep. Prog. Phys. **76**, 046602 (2013).

[10] A. J. Bray, S. N. Majumdar, and G. Schehr, Adv. Phys. **62**, 225 (2013).

[11] R. Metzler, J.-H. Jeon, A. G. Cherstvy, and E. Barkai, Phys. Chem. Chem. Phys. **16**, 24128 (2014).

[12] Y. Meroz and I. M. Sokolov, Phys. Rep. **573**, 1 (2015).

[13] K. Burnecki, E. Kepten, Y. Garini, G. Sikora, and A. Weron, Sci. Rep. **5**, 11306 (2015).

[14] M. Javanainen, H. Hammaren, L. Monticelli, J.-H. Jeon, M. S. Miettinen, H. Martinez-Seara, R. Metzler, and I. Vattulainen, Faraday Discuss. **161**, 397 (2013).

[15] J.-H. Jeon, M. Javanainen, H. Martinez-Seara, R. Metzler, and I. Vattulainen, Phys. Rev. X **6**, 021006 (2016).

[16] L. F. Richardson, Proc. R. Soc. London, Ser. A **110**, 709 (1926).

[17] G. K. Batchelor, Math. Proc. Cambridge Philos. Soc. **48**, 345 (1952).

[18] P. Siegle, I. Goychuk, and P. Hänggi, Phys. Rev. Lett. **105**, 100602 (2010).

[19] H. Berry and H. Chate, Phys. Rev. E **89**, 022708 (2014).

[20] F. Trovato and V. Tozzini, Biophys. J. **107**, 2579 (2014).

[21] M. Weiss, Intl. Rev. Cell Mol. Biol. **307**, 383 (2014).

[22] M. J. Saxton, J. Phys. Chem. B **118**, 12805 (2014).

[23] T. Kühn, T. O. Ihalainen, J. Hyvaluoma, N. Dross, S. F. Willman, J. Langowski, M. Vihinen-Ranta, and J. Timonen, PLoS One **6**, e22962 (2011).

[24] B. P. English, V. Hauryliuk, A. Sanamrad, S. Tankov, N. H. Dekker, and J. Elf, Proc. Natl. Acad. Sci. USA **108**, E365 (2011).

[25] S. Ghosh, A. G. Cherstvy, D. S. Grebenkov, and R. Metzler, New. J. Phys. **18**, 013027 (2016).

[26] I. M. Tolic-Norrelykke, E.-L. Munteanu, G. Thon, L. Oddershede, and K. Berg-Sorensen, Phys. Rev. Lett. **93**, 078102 (2004).

[27] D. Banks and C. Fradin, Biophys. J. **89**, 2960 (2005).

[28] I. Golding and E. C. Cox, Phys. Rev. Lett. **96**, 098102 (2006).

[29] J. Szymanski and M. Weiss, Phys. Rev. Lett. **103**, 038102 (2009).

[30] I. Bronstein, Y. Israel, E. Kepten, S. Mai, Y. Shav-Tal, E. Barkai, and Y. Garini, Phys. Rev. Lett. **103**, 018102 (2009).

[31] S. C. Weber, A. J. Spakowitz, and J. A. Theriot, Phys. Rev. Lett. **104**, 238102 (2010).

[32] K. Burnecki, E. Kepten, J. Janczura, I. Bronshtein, Y. Garini, and A. Weron, Biophys. J. **103**, 1839 (2012).

[33] T. Lebeaupin, H. Sellou, G. Timinszky, and S. Huet, AIMS Biophys. **2**, 458 (2015).

[34] Y. He, S. Burov, R. Metzler, and E. Barkai, Phys. Rev. Lett. **101**, 058101 (2008).

[35] G. Seisenberger, M. U. Ried, T. Endress, H. Brüning, M. Hallek, and C. Bräuchle, Science **294**, 1929 (2001).

[36] J.-H. Jeon, V. Tejedor, S. Burov, E. Barkai, C. Selhuber-Unkel, K. Berg-Sørensen, L. Oddershede, and R. Metzler, Phys. Rev. Lett. **106**, 048103 (2011).

[37] S. M. A. Tabei, S. Burov, H. Y. Kim, A. Kuznetsov, T. Huynh, J. Jureller, L. H. Philipson, A. R. Dinner, and N. F. Scherer, Proc. Natl. Acad. Sci. USA **110**, 4911 (2013).

[38] P. Schwille, U. Haupts, S. Maiti, and W. W. Webb, Biophys. J. **77**, 2251 (1999).

[39] K. Ritchie, X.-Y. Shan, J. Kondo, K. Iwasawa, T. Fujiwara, and A. Kusumi, Biophys. J. **88**, 2266 (2005).

[40] J. Ehrig, E. P. Petrov, and P. Schwille, New J. Phys. **13**, 045019 (2011).

[41] J. Ehrig, E. P. Petrov, and P. Schwille, Biophys. J. **100**, 80 (2011).

[42] G. R. Kneller, K. Baczynski, and M. Pasenkiewicz-Gierula, J. Chem. Phys. **135**, 141105 (2011); S. Stachura and G. R. Kneller, Mol. Simul. **40**, 245 (2014).

[43] M. Hellmann, D. W. Heermann, and M. Weiss, Europhys. Lett. **94**, 18002 (2011).

[44] M. P. Horton, F. Höfling, J. O. Rädler, and T. Franosch, Soft Matter **6**, 2648 (2010).

[45] J.-H. Jeon, H. Martinez-Seara Monne, M. Javanainen, and R. Metzler, Phys. Rev. Lett. **109**, 188103 (2012).

[46] J. E. Goose and M. S. P. Sansom, PLoS Comput. Biol. **9**, e1003033 (2013).

[47] R. Metzler, J.-H. Jeon, and A. G. Cherstvy, Biochem. Biophys. Acta **1858**, 2451 (2016).

[48] E. Yamamoto, A. C. Kalli, T. Akimoto, K. Yasuoka, and M. S. P. Sansom, Sci. Rep. **5**, 18245 (2015).

[49] A. V. Weigel, B. Simon, M. M. Tamkun, and D. Krapf, Proc. Natl. Acad. Sci. USA **108**, 6438 (2011).

[50] G. Campagnola, K. Nepal, B. W. Schroder, O. B. Peersen, and D. Krapf, Sci. Rep. **5**, 17721 (2015).

[51] D. Krapf, Curr. Top. Membranes **75**, 167 (2015).

[52] C. Manzo, J. A. Torreno-Pina, P. Massignan, G. J. Lapeyre, Jr., M. Lewenstein, and M. F. Garcia Parajo, Phys. Rev. X **5**, 011021 (2015).

[53] Y. von Hansen, S. Gekle, and R. R. Netz, Phys. Rev. Lett. **111**, 118103 (2013).

[54] E. Yamamoto, T. Akimoto, M. Yasui, and K. Yasuoka, Sci. Rep. **4**, 4720 (2014).

[55] M. G. Wolf, H. Grubmüller, and G. Grönhof, Biophys. J. **107**, 76 (2014).

[56] C. Chipot and J. Comer, Sci. Rep. **6**, 35913 (2016).

[57] A. Caspi, R. Granek, and M. Elbaum, Phys. Rev. Lett. **85**, 5655 (2000).

[58] A. Caspi, R. Granek, and M. Elbaum, Phys. Rev. E **66**, 011916 (2002).

[59] J. F. Reverey, J.-H. Jeon, H. Bao, M. Leippe, R. Metzler, and C. Selhuber-Unkel, Sci. Rep. **5**, 11690 (2015).

[60] I. Goychuk, V. O. Kharchenko, and R. Metzler, Phys. Chem. Chem. Phys. **16**, 16524 (2014).

[61] I. Goychuk, V. O. Kharchenko, and R. Metzler, PLoS One **9**, e91700 (2014).

[62] L. G. A. Alves, D. B. Scariot, R. R. Guimaraes, C. V. Nakamura, R. S. Mendes, and H. V. Ribeiro, PLoS One **11**, e0152092 (2016).

[63] E. W. Montroll and G. H. Weiss, J. Math. Phys. **6**, 167 (1965).

[64] H. Scher and E. W. Montroll, Phys. Rev. B **12**, 2455 (1975).

[65] T. Neusius, I. M. Sokolov, and J. C. Smith, Phys. Rev. E **80**, 011109 (2009).

[66] E. Barkai, Phys. Rev. Lett. **90**, 104101 (2003).

[67] J. H. P. Schulz, E. Barkai, and R. Metzler, Phys. Rev. Lett. **110**, 020602 (2013).

[68] J. H. P. Schulz, E. Barkai, and R. Metzler, Phys. Rev. X **4**, 011028 (2014).

[69] T. Akimoto and E. Barkai, Phys. Rev. E **87**, 032915 (2013).

[70] T. Akimoto and T. Miyaguchi, Phys. Rev. E **82**, 030102 (2010).

[71] T. Geisel and S. Thomae, Phys. Rev. Lett. **52**, 1936 (1984).

[72] T. Geisel, J. Nierwetberg, and A. Zacherl, Phys. Rev. Lett. **54**, 616 (1985).

[73] M. W. Deem and D. Chandler, J. Stat. Phys. **76**, 911 (1994).

[74] S. Burov and E. Barkai, Phys. Rev. Lett. **98**, 250601 (2007).

[75] C. Monthus and J.-P. Bouchaud, J. Phys. A: Math. Gen. **29**, 3847 (1996).

[76] E. M. Bertin and J.-P. Bouchaud, Phys. Rev. E **67**, 026128 (2003).

[77] M. Dentz *et al.*, Adv. Water Resour. **49**, 13 (2012).

[78] A. V. Chechkin, R. Gorenflo, and I. M. Sokolov, J. Phys. A: Math. Gen. **38**, L679 (2005).

[79] A. Fulinski, Phys. Rev. E **83**, 061140 (2011).

[80] A. Fulinski, J. Chem. Phys. **138**, 021101 (2013).

[81] A. Fulinski, Acta Phys. Pol. **44**, 1137 (2013).

[82] A. G. Cherstvy, A. V. Chechkin, and R. Metzler, New J. Phys. **15**, 083039 (2013).

[83] A. G. Cherstvy, A. V. Chechkin, and R. Metzler, J. Phys. A: Math. Theor. **47**, 485002 (2014).

[84] A. G. Cherstvy and R. Metzler, Phys. Rev. E **90**, 012134 (2014).

[85] A. G. Cherstvy and R. Metzler, J. Stat. Mech. (2015) P05010.

[86] R. Kazakevicius and J. Ruseckas, Phys. Rev. E **94**, 032109 (2016).

[87] M. V. Chubynsky and G. W. Slater, Phys. Rev. Lett. **113**, 098302 (2014).

[88] P. Massignan, C. Manzo, J. A. Torreno-Pina, M. F. Garcia-Parajo, M. Lewenstein, and G. J. Lapeyre, Phys. Rev. Lett. **112**, 150603 (2014).

[89] A. G. Cherstvy and R. Metzler, Phys. Chem. Chem. Phys. **18**, 23840 (2016).

[90] F. Black and M. Scholes, J. Polit. Econ. **81**, 637 (1973).

[91] A. W. C. Lau and T. C. Lubensky, Phys. Rev. E **76**, 011123 (2007).

[92] E. Aghion, D. Vinod, A. G. Cherstvy, A. V. Chechkin, and R. Metzler (unpublished).

[93] Ya. G. Sinai, Theory Probab. Its Appl. **27**, 256 (1982).

[94] A. Godec, A. V. Chechkin, E. Barkai, H. Kantz, and R. Metzler, J. Phys. A: Math. Theor. **47**, 492002 (2014).

[95] A. Bodrova, A. V. Chechkin, A. G. Cherstvy, and R. Metzler, Phys. Chem. Chem. Phys. **17**, 21791 (2015).

[96] A. Bodrova, A. V. Chechkin, A. G. Cherstvy, and R. Metzler, New J. Phys. **17**, 063038 (2015).

[97] M. A. Lomholt, L. Lizana, R. Metzler, and T. Ambjörnsson, Phys. Rev. Lett. **110**, 208301 (2013).

[98] W. Deng and E. Barkai, Phys. Rev. E **79**, 011112 (2009).

[99] M. Schwarzl, A. Godec, and R. Metzler (unpublished).

[100] E. Geneston, R. Tuladhar, M. T. Beig, M. Bologna, and P. Grigolini, Phys. Rev. E **94**, 012136 (2016).

[101] V. Tejedor and R. Metzler, J. Phys. A: Math. Theor. **43**, 082002 (2010).

[102] A. V. Chechkin, M. Hofmann, and I. M. Sokolov, Phys. Rev. E **80**, 031112 (2009).

[103] M. Magdziarz, R. Metzler, W. Szczotka, and P. Zebrowski, Phys. Rev. E **85**, 051103 (2012).

[104] S. C. Lim and S. V. Muniandy, Phys. Rev. E **66**, 021114 (2002).

[105] J.-H. Jeon, A. V. Chechkin, and R. Metzler, Phys. Chem. Chem. Phys. **16**, 15811 (2014).

[106] F. Thiel and I. M. Sokolov, Phys. Rev. E **89**, 012115 (2014).

[107] H. Safdari, A. V. Chechkin, G. R. Jafari, and R. Metzler, Phys. Rev. E **91**, 042107 (2015).

[108] H. Safdari, A. G. Cherstvy, A. V. Chechkin, F. Thiel, I. M. Sokolov, and R. Metzler, J. Phys. A: Math. Theor. **48**, 375002 (2015).

[109] A. Bodrova, A. V. Chechkin, A. G. Cherstvy, H. Safdari, I. M. Sokolov, and R. Metzler, Sci. Rep. **6**, 30520 (2016).

[110] G. Guigas, C. Kalla, and M. Weiss, Biophys. J. **93**, 316 (2007).

[111] L. L. Latour, K. Svoboda, P. Mitra, and C. H. Sotak, Proc. Natl. Acad. Sci. USA **91**, 1229 (1994).

[112] N. V. Brilliantov and T. Pöschel, Phys. Rev. E **61**, 1716 (2000).

[113] N. V. Brilliantov and T. Pöschel, *Kinetic Theory of Granular Gases* (Oxford University Press, Oxford, 2004).

[114] T. Miyaguchi, T. Akimoto, and E. Yamamoto, Phys. Rev. E **94**, 012109 (2016).

[115] T. Akimoto and E. Yamamoto, Phys. Rev. E **93**, 062109 (2016).

[116] R. Rozenfeld, J. Luczka, and P. Talkner, Phys. Lett. A **249**, 409 (1998); J. Luczka, P. Talkner, and P. Hänggi, Phys. A (Amsterdam) **278**, 18 (2000); J. Luczka, M. Niemec, and E. Piotrowski, Phys. Lett. A **167**, 475 (1992); J. Phys. A: Math. Gen. **26**, 4849 (1993).

[117] G. E. Uhlenbeck and L. S. Ornstein, Phys. Rev. **36**, 823 (1930).

[118] J.-H. Jeon and R. Metzler, Phys. Rev. E **81**, 021103 (2010); I. Goychuk, *ibid.* **80**, 046125 (2009).

[119] J.-H. Jeon and R. Metzler, Phys. Rev. E **85**, 021147 (2012).

[120] R. Metzler and J. Klafter, J. Phys. Chem. B **104**, 3851 (2000).

[121] E. Barkai and R. J. Silbey, J. Phys. Chem. B **104**, 3866 (2000).

[122] G. A. Pavliotis and A. Vogiannou, Fluct. Noise Lett. **08**, L155 (2008).

[123] G. Antczak and G. Ehrlich, Phys. Rev. B **71**, 115422 (2005).

[124] S. Hallerberg and A. S. de Wijn, Phys. Rev. E **90**, 062901 (2014).

[125] M. Henkel, M. Pleimling, and R. Sanctuary, *Aging and the Glass Transition* (Springer, Berlin, 2007).

[126] L. C. E. Struik, *Physical Aging in Amorphous Polymers and Other Materials* (Elsevier, Amsterdam, 1978).

[127] E.-J. Donth, *The Glass Transition* (Springer, Berlin, 2001).

[128] H. Krüsemann, R. Schwarzl, and R. Metzler, Transp. Porous Media **115**, 327 (2016).

[129] H. Tanaka, S. Jabbari-Farouji, J. Meunier, and D. Bonn, Phys. Rev. E **71**, 021402 (2005).

[130] R. E. Courtland and E. R. Weeks, J. Phys.: Condens. Matter **15**, S359 (2003).

[131] P. Wang, C. Song, and H. A. Makse, Nat. Phys. **2**, 526 (2006).

[132] S. Boettcher and P. Sibani, J. Phys.: Condens. Matter **23**, 065103 (2011).

[133] D. El Masri, L. Berthier, and L. Cipelletti, Phys. Rev. E **82**, 031503 (2010).

[134] J. J. Brey, A. Prados, M. I. Garca de Soria, and P. Maynar, J. Phys. A: Math. Gen. **40**, 14331 (2007).

[135] A. V. Weigel, M. M. Tamkun, and D. Krapf, Proc. Natl. Acad. Sci. USA **110**, E4591 (2013).

[136] R. Metzler, Nat. Phys. **12**, 113 (2016).

[137] X. Hu, L. Hong, M. D. Smith, T. Neusius, X. Cheng, and J. C. Smith, Nat. Phys. **12**, 171 (2016).

[138] M. Schubert, E. Preis, J. C. Blakesley, P. Pingel, U. Scherf, and D. Neher, Phys. Rev. B **87**, 024203 (2013).

[139] F. D. Stefani, J. P. Hoogenboom, and E. Barkai, Phys. Today **62**(2), 34 (2009).

[140] G. Margolin and E. Barkai, Phys. Rev. Lett. **94**, 080601 (2005).

[141] Y. M. Wang, R. H. Austin, and E. C. Cox, Phys. Rev. Lett. **97**, 048302 (2006).

[142] J.-P. Bouchaud, J. Phys. I **2**, 1705 (1992).

[143] G. Bel and E. Barkai, Phys. Rev. Lett. **94**, 240602 (2005).

[144] A. Rebenshtok and E. Barkai, Phys. Rev. Lett. **99**, 210601 (2007).

[145] J. L. Lebowitz and O. Penrose, Phys. Today **26**(2), 23 (1973).

[146] A. Lubelski, I. M. Sokolov, and J. Klafter, Phys. Rev. Lett. **100**, 250602 (2008).

[147] S. M. Rytov, Yu. A. Kravtsov, and V. I. Tatarskii, *Principles of Statistical Radiophysics 1: Elements of Random Process Theory* (Springer, Heidelberg, 1987).

[148] T. Uneyama, T. Miyaguchi, and T. Akimoto, Phys. Rev. E **92**, 032140 (2015).

[149] M. Abramowitz and I. A. Stegun, *Handbook of Mathematical Functions*, National Bureau of Standards, Washington, DC (Dover, New York, 1972).

[150] N. Van Kampen, *Stochastic Processes in Physics and Chemistry*, 3rd ed. (Elsevier, Amsterdam, 2007).

[151] H. Risken and T. Frank, *The Fokker-Planck Equation: Methods of Solution and Applications* (Springer, Berlin, 1996).

[152] J.-H. Jeon and R. Metzler, J. Phys. A: Math. Theor. **43**, 252001 (2010).

[153] J. Kursawe, J. Schulz, and R. Metzler, Phys. Rev. E **88**, 062124 (2013).

[154] J.-H. Jeon, N. Leijnse, L. B. Oddershede, and R. Metzler, New J. Phys. **15**, 045011 (2013).